Fast three-dimensional phase-unwrapping algorithm based on sorting by reliability following a non-continuous path

Hussein Abdul-Rahman*, Munther Gdeisat*, David Burton* and Michael Lalor*
*General Engineering Research Institute (GERI), Liverpool John Moores University,
Liverpool L3 3AF, U.K.

ABSTRACT

In this paper, we propose a novel three-dimensional phase unwrapping algorithm that extends the "two-dimensional phase unwrapping algorithm based on sorting by reliability following a non-continuous path" into three dimensions. The proposed algorithm depends on a quality map to unwrap the more reliable voxels first and the less reliable ones last. It follows a non-continuous path to perform the unwrapping process. Computer simulation has demonstrated that the proposed algorithm is more suitable than its two dimensional counterpart when used to unwrap volumetric data.

Keywords: Fringe pattern analysis, phase unwrapping.

1. INTRODUCTION

Phase unwrapping has applications in many advanced imaging technologies such as optical interferometry, satellite radar interferometry (SAR), and magnetic resonance imaging (MRI) where the required data is encoded in the form of a phase distribution. The measured phase is normally wrapped between $-\pi$ and π. The wrapped phase is not usable until the 2π phase discontinuities are resolved using a phase unwrapping algorithm.

Many two-dimensional phase unwrapping algorithms have been proposed during the last decade, and many of journal papers have been published and the field now has its own textbook [1]. These algorithms vary in their quality and computational intensity requirements.

Arevallilo Herraez et al. have proposed a two-dimensional phase unwrapping algorithm that depends on a quality map to unwrap a wrapped phase map. It unwraps the pixels of highest quality first and the pixels of lowest quality last and it follows a non-continuous path to perform the unwrapping process [2]. This algorithm is very robust and fast and has been used in building a robust fringe pattern analysis system for human body shape measurement [3].

Many applications produce three-dimensional wrapped phase volumes such as the non-contact measurement of dynamic objects [4], multitemporal SAR interferometric measurements [5] and MRI [6]. A wrapped phase volume can be visualized as a number of consecutive two-dimensional wrapped phase maps. Each map can be unwrapped individually using a two-dimensional phase unwrapping algorithm [7].

A few three-dimensional phase unwrapping algorithms have been proposed recently. Huntley investigated the three-dimensional phase unwrapping problem and demonstrated that a unique solution exists and could be achieved using his phase unwrapping algorithm [4]. This is in contrast to the two-dimensional phase unwrapping algorithms where no unique solution exists. Also, different two-dimensional phase unwrapping algorithms may produce different results when unwrapping the same wrapped phase map [1]. Other robust three-dimensional phase unwrapping algorithms have been proposed by Costantini et al. [5], and Cusack and Papadakis [6]. It is worth mentioning that three-dimensional phase unwrapping algorithms are different from temporal phase unwrapping techniques [8].

Huntley's and Costantini's algorithms are global techniques and normally require long execution times. Cusack and Papadakis have developed a path-following algorithm to unwrap MRI images and their algorithm requires, relatively, a moderate execution time.

Optical Measurement Systems for Industrial Inspection IV, edited by Wolfgang Osten,
Christophe Gorecki, Erik Novak, Proc. of SPIE Vol. 5856 (SPIE, Bellingham, WA, 2005)
0277-786X/05/$15 · doi: 10.1117/12.611415

In this paper, we propose a novel three-dimensional phase unwrapping algorithm that extends Arevallilo Herraez's algorithm into three-dimensions [2]. The proposed algorithm determines the reliability of voxels using the second difference algorithm. Then it follows a discrete path to unwrap the highest quality voxels with the highest reliability values first and the lowest quality voxels with the lowest reliability values last to prevent error propagation. Despite the possibility of some unwrapping errors remaining undetected and propagating in a manner that depends on the unwrapping path; the algorithm is surprisingly robust as will be demonstrated below. Also, the proposed algorithm is more robust and accurate than its two-dimensional counterpart since the three-dimensional space provides more choices of paths than the two-dimensional one.

2. ALGORITHM

Initially the algorithm calculates the reliability of each voxel using the second difference algorithm. Voxels are the constructing elements of a three-dimensional phase volume, similar to pixels in a two-dimensional phase map.

As mentioned before, this algorithm extends the two-dimensional phase unwrapping algorithm based on sorting the reliability following a non-continuous path into three dimensions [2]. The algorithm follows discrete paths to unwrap the highest quality voxels with the highest reliability values first and the lowest quality voxels with the lowest reliability values last to prevent error propagation. The reliability of a pixel in a two-dimensional wrapped phase map can be calculated using its 8 direct neighbouring pixels [2]. Similarly, the reliability of a voxel in a wrapped phase volume can be computed using its 26 direct neighbouring voxels. The three-dimensional phase unwrapping algorithm tends to follow the best path to unwrap the wrapped phase volume.

The proposed algorithm can be outlined in the following steps:

- Determine the reliability of all voxels except the voxels at the border surfaces.
- Calculate the horizontal, vertical and normal edges' reliability.
- Sort all of these edges according to their reliabilities.
- Unwrap voxels according to the edges reliabilities; so that the voxels which connect the highest reliable edges are unwrapped first.
- Unwrap the border surfaces.

Determining the Reliability of a voxel:

Different criteria already exist to construct a quality map such as phase derivative variance, maximum phase gradient and second phase difference [1]. This quality map is derived from the wrapped phase. In this paper, we choose the second difference algorithm to determine the quality of voxels.

In two-dimensional wrapped phase maps, the quality of a pixel is calculated using its surrounding pixels. For example, to calculate the quality of a pixel using a 3×3 window, the pixel and its eight neighbours are taken into consideration as explained in ref [2]. Similarly, to calculate the quality of a voxel in a three-dimensional phase volume, the voxel and its 26 surrounding voxels are considered as shown in Fig. 1.

To calculate the quality of a voxel using the second difference algorithm, the second differences between the voxel and its neighbours are calculated first using equation (1).

$$D(i,j,k) = \left[H^2(i,j,k) + V^2(i,j,k) + N^2(i,j,k) + \sum_{n=1}^{10} D_n^2(i,j,k) \right]^{\frac{1}{2}} \quad (1)$$

Where,

$$
\begin{aligned}
H(i,j,k) &= \gamma\left[\varphi(i-1,j,k)-\varphi(i,j,k)\right]-\gamma\left[\varphi(i,j,k)-\varphi(i+1,j,k)\right]\\
V(i,j,k) &= \gamma\left[\varphi(i,j-1,k)-\varphi(i,j,k)\right]-\gamma\left[\varphi(i,j,k)-\varphi(i,j+1,k)\right]\\
N(i,j,k) &= \gamma\left[\varphi(i,j,k-1)-\varphi(i,j,k)\right]-\gamma\left[\varphi(i,j,k)-\varphi(i,j,k+1)\right]\\
D_1(i,j,k) &= \gamma\left[\varphi(i-1,j-1,k)-\varphi(i,j,k)\right]-\gamma\left[\varphi(i,j,k)-\varphi(i+1,j+1,k)\right]\\
D_2(i,j,k) &= \gamma\left[\varphi(i+1,j-1,k)-\varphi(i,j,k)\right]-\gamma\left[\varphi(i,j,k)-\varphi(i-1,j+1,k)\right]\\
D_3(i,j,k) &= \gamma\left[\varphi(i-1,j-1,k-1)-\varphi(i,j,k)\right]-\gamma\left[\varphi(i,j,k)-\varphi(i+1,j+1,k+1)\right]\\
D_4(i,j,k) &= \gamma\left[\varphi(i,j-1,k-1)-\varphi(i,j,k)\right]-\gamma\left[\varphi(i,j,k)-\varphi(i,j+1,k+1)\right]\\
D_5(i,j,k) &= \gamma\left[\varphi(i+1,j-1,k-1)-\varphi(i,j,k)\right]-\gamma\left[\varphi(i,j,k)-\varphi(i-1,j+1,k+1)\right]\\
D_6(i,j,k) &= \gamma\left[\varphi(i-1,j,k-1)-\varphi(i,j,k)\right]-\gamma\left[\varphi(i,j,k)-\varphi(i+1,j,k+1)\right]\\
D_7(i,j,k) &= \gamma\left[\varphi(i-1,j+1,k-1)-\varphi(i,j,k)\right]-\gamma\left[\varphi(i,j,k)-\varphi(i+1,j-1,k+1)\right]\\
D_8(i,j,k) &= \gamma\left[\varphi(i+1,j,k-1)-\varphi(i,j,k)\right]-\gamma\left[\varphi(i,j,k)-\varphi(i-1,j,k+1)\right]\\
D_9(i,j,k) &= \gamma\left[\varphi(i,j+1,k-1)-\varphi(i,j,k)\right]-\gamma\left[\varphi(i,j,k)-\varphi(i,j-1,k+1)\right]\\
D_{10}(i,j,k) &= \gamma\left[\varphi(i+1,j+1,k-1)-\varphi(i,j,k)\right]-\gamma\left[\varphi(i,j,k)-\varphi(i-1,j-1,k+1)\right]
\end{aligned}
\tag{2}
$$

Where γ(.) is a simple wrapping operation to remove any 2π steps between the consecutive voxels (i.e. $y = \gamma(x)$ is equivalent to $y = (x \bmod 2\pi) - \pi$, where *mod* is the modular operation in digital computers). H, V and N are the horizontal, vertical and normal second differences. D_n is the n^{th} diagonal difference. The reliability $R(i,j,k)$ is calculated using equation (3). The higher the reliability value, the higher the quality of the voxel and vice versa.

$$
R(i,j,k) = \frac{1}{D(i,j,k)} \tag{3}
$$

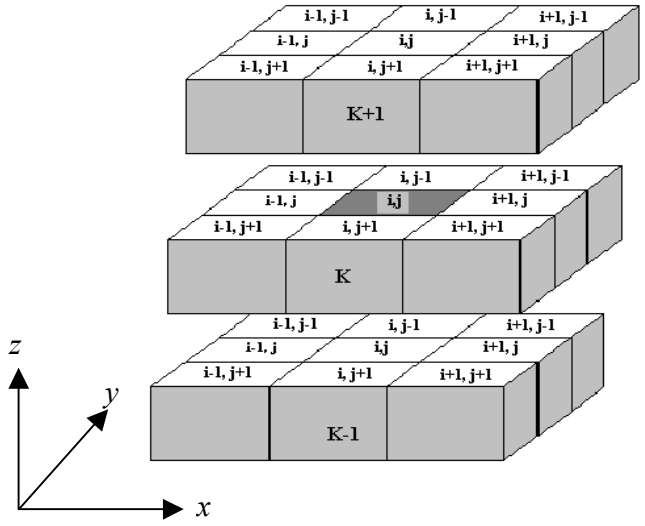

Figure 1: The calculation of the second difference of a voxel using its 26 neighbours.

Unwrapping Path

An edge is an intersection of two voxels that are connected in the x, y or z directions as shown in Fig. 2. Edges can be classified as vertical, horizontal and normal edges. The reliability of an edge is defined as the summation of the reliability of the two voxels that the edge connects as shown in Fig. 3. Since the reliability values of all the voxels in the phase volume can be calculated, the calculation of the reliability of all the edges can be performed for all the edges in the phase volume. The reliability value of an edge that connects a border voxel with another voxel in the phase volume is set to zero.

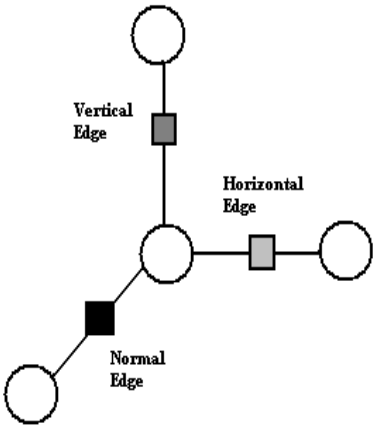

Figure 2: The vertical, horizontal and normal edges.

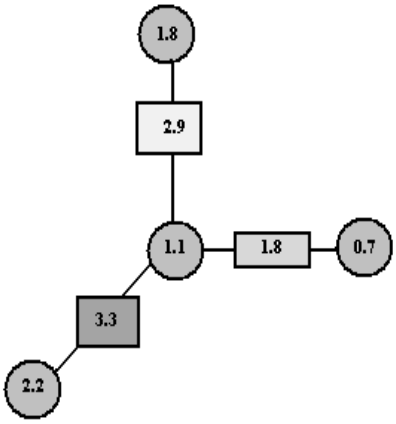

Figure 3: The edges' reliability.

An unwrapping path cannot be defined relative to the reliability of the pixels. Instead it is defined by looking at the value of the reliability of the edges. The definition of the unwrapping path is relatively simple. All the edges are stored in an array and sorted by value of reliability. Those edges with higher reliability are resolved first as will be explained below. The construction of the unwrapping path is similar to the phase unwrapping algorithm in ref. [2] but extended to three dimensions.

Figures 4(a) - 4(i) illustrate the principle of the proposed algorithm. Suppose that we want to unwrap the voxels, whose edges reliability are already sorted and their orders are shown in Fig 4(a). The integer numbers represent the order of edges in the sorted array. The edge that has the order 1 is processed first then the edge with order 2 and so on.

Initially all voxels are considered as not belonging to any group, which is represented by the white circles in Fig. 4(a). Both voxels surrounding the edge with order 1 in Fig. 4(a) are unwrapped first with respect to each other, and both voxels are joined together in single group as illustrated in Fig 4(b). Fig. 4(c) shows more processed voxels, and more groups are formed, but all of those groups are generated from non-grouped voxels.

The voxels forming the edge 6 in Fig. 4(c) are to be processed in this stage. As we can see one of these voxels has its own group but the other pixel does not belong to any group. The ungrouped voxel is unwrapped with respect to the grouped one, and set to be a member of the group as shown in Fig. 4(d).

Edge number 7 in Fig. 4(d) connects two grouped voxels, so in this case the group of fewer members is unwrapped with respect to the group with more members, and both groups merge into a single group as illustrated in Fig. 4(e).

Edges number 15 and 16 in Fig 4(e) also connect voxels with different groups, so their groups are unwrapped with respect to each other according to the number of members and their groups and merged together as shown in Fig. 4(f). This process is continued as shown in Figs. 4(g)-4(i), until all of the voxels have been unwrapped and all now belong to the same group as illustrated in Fig. 4(i). Note that unwrapping a pixel or a group of pixels with respect to another group may require the addition or subtraction of multiples of 2π.

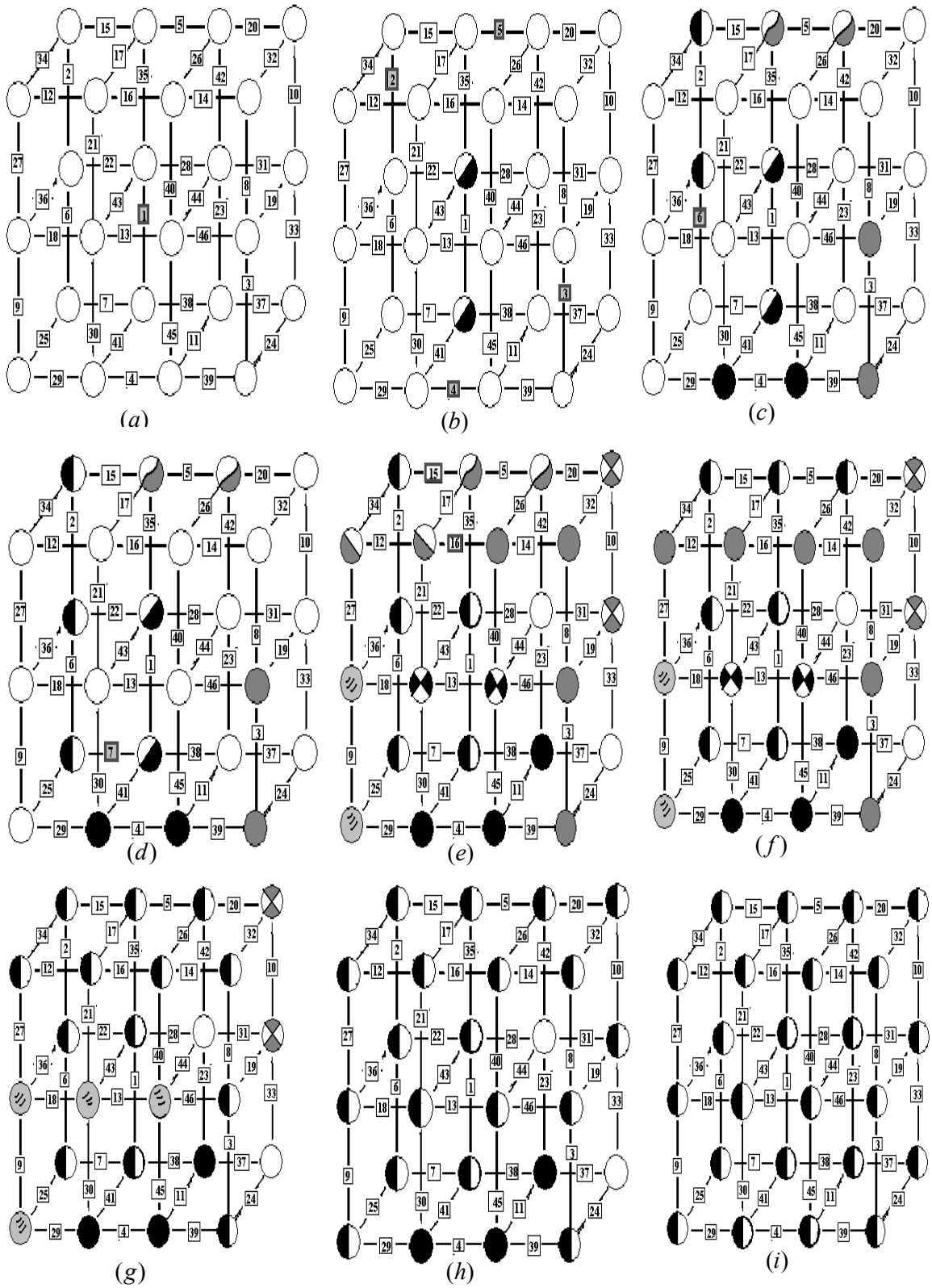

Figure 4: Demonstration of the proposed algorithm.

The proposed phase unwrapping can be summarised as follows:

1- If both voxels do not belong to any group and have not been unwrapped before; the voxels are unwrapped with respect to each other and gathered into a single group.
2- If one of the voxels has been processed before and belongs to a group but the other has not, then the voxel that has not been processed before is unwrapped with respect to the other voxels in the group and now joins this group.
3- If both voxels have been processed before and both belong to different groups, then the two groups are unwrapped with respect to each other. The smallest group is unwrapped with respect to the largest group. Then the two groups are joined together to construct a single group.

3. SIMULATED RESULTS

The proposed algorithm has been tested using a computer simulation in order to examine its validity and compare its performance to its two-dimensional counterpart technique. Two test objects have been used to test the algorithm. The first object is a planar surface, which is shown in Fig. 5(a) in three-dimensional representation. Also the surface is shown in grey scale in Fig. 5(b). The object has been scaled between the black and white colours for display purposes. The white colour represents the maximum height of the object and the black colour represents its minimum height. The object can be described by the equation $z_{i,j,k} = 0.1\ (x_{i,j,k} + y_{i,j,k})$. Where z is the height of the object. The image of the simulated object consists of 256 × 256 pixels. The object moves up slowly as described by the equation below.

$$z_{i,j,k,t} = 0.1(x_{i,j,k} + y_{i,j,k,t}) + 0.1\ t \tag{4}$$

Where t represents the time in seconds. Assume that 100 frames of fringe patterns are grabbed during a 100 sec period. Consequently, the height difference between two successive frames is 0.1 units. All the frames have been corrupted using Gaussian noise and the resultant frames have been wrapped between π and -π. The frame at t = 99 sec is shown in Fig. 6(a). All the frames have been unwrapped individually using the two-dimensional phase unwrapping algorithm described in ref. [2] and the unwrapped phase map produced at t = 99 sec is shown in Fig. 6(b). The proposed 3D algorithm has unwrapped the phase volume and the frame at the time instant t = 99 sec is shown in Fig. 6(c). The comparison of Figs. 6(b) & 6(c) revealed that the proposed algorithm outperforms its two-dimensional counterpart.

The same procedure was repeated using a more complicated object, which has a very steep surface as shown in Fig. (7). This object moves up slowly and can be described by the following equation:

$$\begin{aligned} z_{i,j,k,t} = {} & 2.448\left[\left(1-x^2_{i,j,k}\right)\exp\left(-x^2_{i,j,k}-\left(y_{i,j,k}+1\right)^2\right)\right]-8.16\left[\left(\frac{x_{i,j,k}}{5}-x^3_{i,j,k}-y^5_{i,j,k}\right)\exp\left(-x^2_{i,j,k}-y^2_{i,j,k}\right)\right] \\ & -0.272\left[\exp\left(-\left(x_{i,j,k}+1\right)^2-y^2_{i,j,k}\right)\right]+0.1(x_{i,j,k}+y_{i,j,k})+(0.1\ t) \end{aligned} \tag{5}$$

Where $z_{i,j,k}$ is the height of the point (i,j,k) at time t, where $0 \le t \le 99$ sec. The object has been corrupted with Gaussian noise and the resultant shape has been wrapped between π and -π. The frame at the time instant t = 99 sec is shown in Fig. 8(a). All the frames have been unwrapped individually using the two-dimensional phase unwrapping algorithm described in ref. [2] and the unwrapped phase map produced at t = 99 sec is shown in Fig. 8(b). The proposed 3D algorithm has unwrapped the phase volume and the frame at the time instant t = 99 sec is shown in Fig. 8(c). By comparing Figs. 8(b) & 8(c), we can conclude that the proposed algorithm outperforms its two-dimensional counterpart.

The proposed algorithm has been implemented using the C programming language. The algorithm has been executed on a PC with Pentium 4 processor that runs at 3.2 GHz clock speed. The memory of the PC is 4G-Byte RAM. The execution time to unwrap a phase volume of 256 × 256 × 100 voxels is approximately seven minutes.

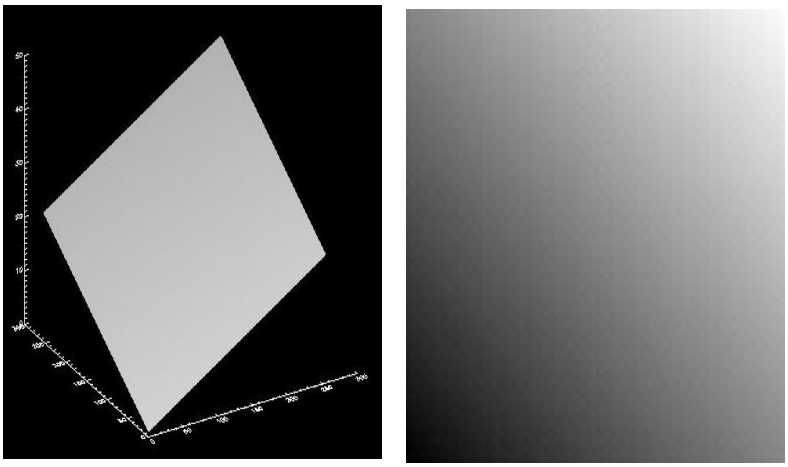

(a) (b)

Figure 5: A simulated plane object at t = 0.

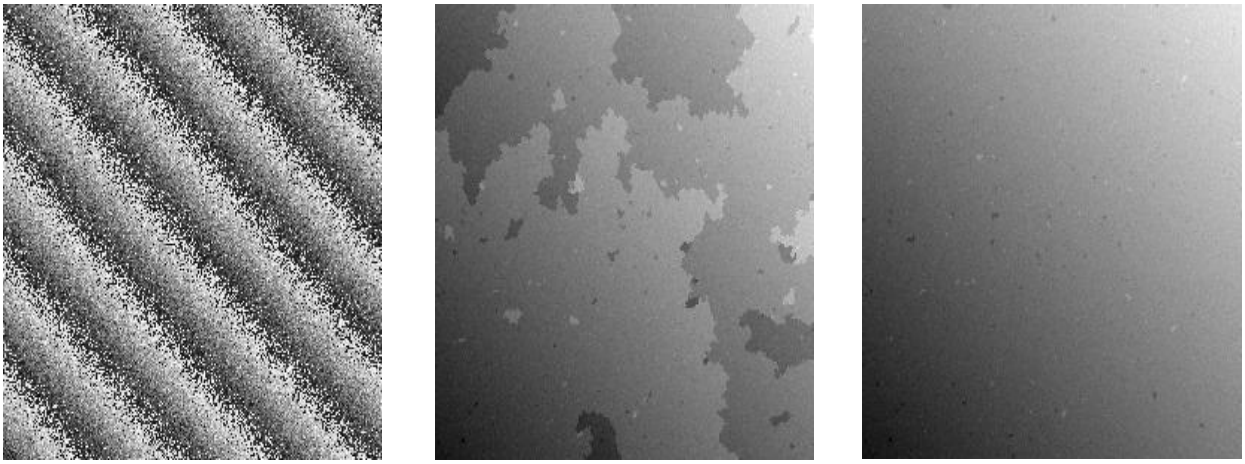

(a) (b) (c)

Figure 6: (a) Wrapped phase distribution for the planar object at t = 99 corrupted with high level of noise. (b) Unwrapped phase distribution of (a) using the 2D phase unwrapping algorithm. (c) unwrapped phase distribution of (a) using the 3D phase unwrapping algorithm.

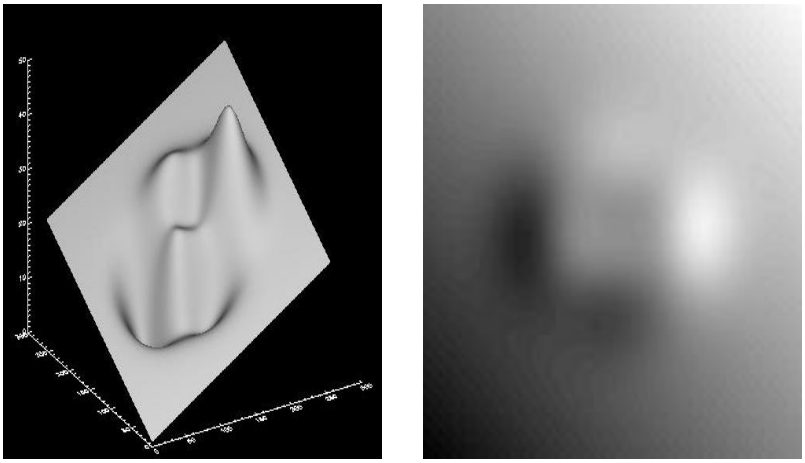

(a) (b)

Figure 7: A test object with steep surface.

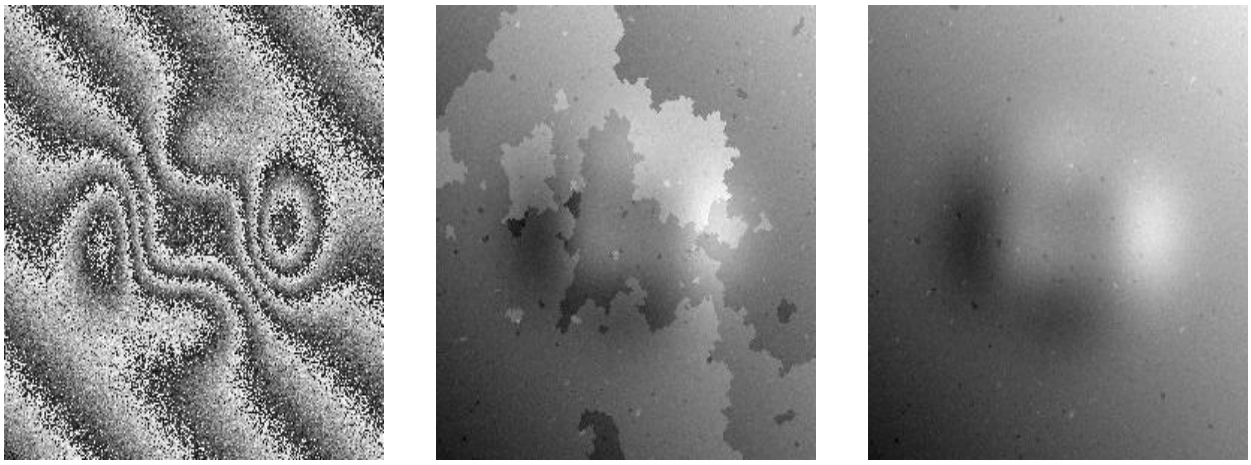

(a) (b) (c)

Figure 8:(a) Wrapped phase distribution for the object shown in Fig. 7(a) at t=99 corrupted with a high level of noise. (b) Unwrapped phase distribution of (a) using the 2D phase unwrapping algorithm. (c) unwrapped phase distribution of (a) using the 3D phase unwrapping algorithm.

4. CONCLUSIONS

A novel three-dimensional phase unwrapping algorithm has been described and tested using computer simulation. Simple planar and complicated objects have been used to examine the validity of the algorithm and compare its performance with its two-dimensional counterpart. Computer simulation has demonstrated that the algorithm can perform well against noise and it outperforms its two-dimensional counterpart. This three-dimensional unwrapping algorithm demonstrates the principle that unwrapping a phase volume using three-dimensional phase maps produce better results than unwrapping each frame in the phase volume individually using two-dimensional algorithms.

REFERENCES

1. D. Ghiglia, and M. Pritt. "*Two dimensional phase unwrapping; theory, algorithms and software*," John Wiley & Sons, 1998.
2. M. Arevallilo Herraez, D. Burton, M. Lalor, and M. Gdeisat, "Fast two-dimensional phase-unwrapping algorithm based on sorting by reliability following a non-continuous path," *Appl. Opt.* **41**, pp. 7437-7444, 2002.
3. F. Lilley, M. Lalor, and D. Burton, "Robust fringe analysis system for human body shape measurement," *Optical Engineering*. **39**, pp. 187-195, 2000.
4. J. Huntly, "Three-Dimensional noise-immune phase unwrapping algorithm," *App.l Opt*. **41**, pp. 3091-3100, 2001.
5. M. Costanitini, F. Malvarosa, L. Minati, and G. Milillo, "A three dimensional phase unwrapping algorithm for processing of multitemporal SAR interferometric measurements," *IEEE transaction on Geoscience and Remote sensing*. **40**, pp. 1741-1743, 2002.
6. R. Cusack, and N. Papadakis, "New robust 3-D phase unwrapping algorithms: application to magnetic field mapping and undistorting echoplanar images," *NeuroImage*. **16**, pp. 754-764, 2001.
7. X. Su, W. Chen, Q. Zhang, and Y. Chao "Dynamic 3D-shape measurement method based on FTP," *Optics and Lasers in Engineering*. **36**, pp. 49-64, 2001.
8. J. Huntley, and H. Saldner, "Temporal phase-unwrapping algorithm for automated interferogram analysis," *Appl. Opt*. **32**, pp. 3047-3052, 1993.